



Published in final edited form as:

*Mol Cancer Res.* 2008 June ; 6(6): 937–946. doi:10.1158/1541-7786.MCR-07-2115.

## Cell Cycle Regulator Gene *CDC5L*, a Potential Target for 6p12-p21 Amplicon in Osteosarcoma

Xin-Yan Lu<sup>1,3</sup>, Yaojuan Lu<sup>1</sup>, Yi-Jue Zhao<sup>1</sup>, Kim Jaeweon<sup>4</sup>, Jason Kang<sup>4</sup>, Li Xiao-Nan<sup>1</sup>, Gouqing Ge<sup>1</sup>, Rene Meyer<sup>1</sup>, Laszlo Perlaky<sup>1</sup>, John Hicks<sup>2</sup>, Murali Chintagumpala<sup>1</sup>, Wei-Wen Cai<sup>3</sup>, Marc Ladanyi<sup>5</sup>, Richard Gorlick<sup>6</sup>, Ching C. Lau<sup>1</sup>, Debananda Pati<sup>1</sup>, Michael Sheldon<sup>1</sup>, and Pulivarthi H. Rao<sup>1</sup>

<sup>1</sup>Department of Pediatrics, Baylor College of Medicine

<sup>2</sup>Department of Pathology, Baylor College of Medicine

<sup>3</sup>Department of Molecular and Human Genetics, Baylor College of Medicine

<sup>4</sup>Spectral Genomics, Houston, Texas

<sup>5</sup>Memorial Sloan Kettering Cancer Center, New York, New York

<sup>6</sup>The Children's Hospital at Montefiore, Bronx, New York

### Abstract

Osteosarcoma is a primary malignant tumor of bone arising from primitive bone-forming mesenchymal cells and accounts for ~60% of malignant bone tumors. Our comparative genomic hybridization (CGH) studies have identified frequent amplification at 6p12-p21, 12q13-q15, and 17p11.2 in osteosarcoma. Of these amplified regions, 6p12-p21 is particularly interesting because of its association with progression and poor prognosis in patients with osteosarcoma. In an attempt to identify aberrantly expressed gene(s) mapping to the 6p12-p21 amplicon, a region-specific array was generated using 108 overlapping BAC and P1 clones covering a 28.8-Mb region at 0.26-Mb intervals. Based on array CGH analysis, the 6p amplicon was refined to 7.9 Mb between the clones RP11-91E11 and RP1-244F2 and 10 amplified clones, with possible target genes, were identified. To study the expression pattern of the target genes from the hotspot amplicon and known candidate genes from 6p12-21, we did quantitative reverse transcription-PCR analysis of MAPK14, MAPK13, CDKN1A, PIM1, MDGA1, BTB9, DNAH8, CCND3, PTK7, CDC5L, and *RUNX2* on osteosarcoma patient samples and seven cell lines. The combined array CGH and quantitative reverse transcription-PCR analysis identified amplification and overexpression of *CDC5L*, *CCND3*, and *RUNX2*. We screened these three genes for protein expression by Western blotting and immunohistochemistry and detected overexpression of *CDC5L*. Furthermore, we used an *in vivo* assay to show that *CDC5L* possesses potential oncogenic activity. These results indicate that *CDC5L*, a cell cycle regulator important for the G<sub>2</sub>-M transition, is the most likely candidate oncogene for the 6p12-p21 amplicon found in osteosarcoma.

---

Copyright © 2008 American Association for Cancer Research.

**Requests for reprints:** Pulivarthi H. Rao, Texas Children's Cancer Center, Baylor College of Medicine, 6621 Fannin Street, MC 3-3320, Houston, TX 77030. Phone: 832-824-4820; Fax: 832-825-4038. E-mail: E-mail: prao@bcm.tmc.edu.  
Current address for M. Sheldon: Department of Genetics, Rutgers University, Piscataway, New Jersey.

**Note:** Supplementary data for this article are available at Molecular Cancer Research Online (<http://mcr.aacrjournals.org/>).

Disclosure of Potential Conflicts of Interest

No potential conflicts of interest were disclosed.

## Introduction

Osteosarcomas are the most frequent malignant bone tumor in adults and children with a peak incidence during the second decade of life (1). Sporadic human osteosarcomas often present with complex chromosomal rearrangements, deletions, and amplifications, suggesting that genomic instability is linked to the development of this tumor (2-8). Exposure to ionizing radiation, for example during radiotherapy of other cancers, is a high-risk factor for development of osteosarcoma at the irradiated site, further suggesting that DNA breakage and genomic instability contribute to the development of this tumor (9). The identification of recurrent amplifications and deletions in human osteogenic tumors may provide genetic evidence for specific sequences that contribute to the malignant phenotype.

Recently, others and we have identified several chromosomal regions that are recurrently amplified in osteosarcoma by chromosomal comparative genomic hybridization (CGH) and array-based CGH (2-8,10). Of these, amplification of 6p12-p21 and 17p11.2 appeared to be markers of an early genetic change in osteosarcoma. The high frequency of copy number increases in these regions suggests the presence of candidate oncogenes that have yet to be identified. The 6p gain/amplicon has also been reported in other tumor types, including bladder and pancreatic cancers, diffuse large B-cell lymphoma, and retinoblastoma (11-14). However, the amplification in these tumors mapped to 6p22, which is telomeric to the amplicon found in osteosarcoma. The 6p12-p21 genomic region is particularly interesting because of its association with poor prognosis in patients with osteosarcoma.<sup>7</sup> To date, no bona fide oncogene sequences have been described in this region of the genome. Therefore, identification of amplified gene(s) from the 6p12-p21 amplicon is extremely important because it not only advances our understanding of tumor initiation but also offers the potential for developing nonsurgical treatments by targeting these molecules through gene therapy or antisense molecules. We recently did array CGH—based copy number analysis on primary osteosarcoma tumors and identified a 9.4-Mb amplicon at 6p12-p21.

To map the boundaries of the 6p12-p21 amplicon more precisely, a region-specific CGH microarray was generated using 108 human BAC and PAC clones, which span a 28.8 Mb region of 6p in osteosarcoma. The analysis of genomic DNAs from osteosarcoma patients with 6p12-p21 amplification using this region-specific array revealed a large amplification “field” covering 7.9 Mb between the clones RP11-91E11 and RP1-244F2, and identified 10 amplified clones with possible target genes. Expression analysis of genes that map within these amplified peaks identified several genes that are up-regulated in primary tumors and cell lines. The combined array CGH and quantitative reverse transcription PCR (qRT-PCR) analysis identified amplification and overexpression of *CDC5L*, *CCND3*, and *RUNX2*. Finally, we investigated whether increased DNA copy number and overexpression of *CCND3*, *CDC5L*, and *RUNX2* transcripts correlates with increased protein levels in osteosarcoma cell lines and tissue microarray. Here, we present results from the detailed mapping of the 6p12-p21 amplicon and expression analysis of genes that are amplified in osteosarcoma.

## Results

### Frequent Amplification of 6p12-p21 in Osteosarcoma

Using chromosomal CGH, we identified several recurrent high-level chromosomal amplifications at Xp11, 1q21, 4q12, 5p14-p15, 6p12-p21, 7p21-p22, 8q22-q23, 12q12-q15, 17p11, and 20p11.2 (7,8). Of these, amplification of 6p12-p21 was not only present at high frequency but was also detected in all specimen types, including those from biopsy, definitive

---

<sup>7</sup>P.H. Rao, et al. Gain of chromosome 7p and 8q23-q24 are associated with poor prognosis in osteosarcoma, unpublished material.

surgery, and metastatic lesions, suggestive of an early event in the pathogenesis of osteosarcoma. Our recent array CGH analysis using 3-Mb arrays identified high-level amplification of the clones from 6p12-p21 in 12 of 48 (25%) of the cases (10). These findings strongly suggest the presence of potential oncogene(s) in the 6p12-p21 region. We used Kaplan-Meier analysis to determine the prognostic significance of the 6p12-p21 amplification in 28 biopsies (11 good responders and 17 poor responders). Amplification of 6p12-p21 was noted in 5 of 28 samples and patients with 6p12-p21 amplification displayed a trend toward shorter event-free survival compared with patients who did not have the amplification.<sup>7</sup>

### Fine Mapping of the 6p12-p21 Amplicon in Osteosarcoma

To further define the 6p12-p21 amplicon, we applied a region-specific CGH array, composed of 108 contiguous BACs and P1 clones covering a 28.8-Mb region at 0.26-Mb intervals, to the analysis of 26 osteosarcomas (Fig. 1A; see Supplementary Data for array CGH). These 26 cases consist of 9 cases with no change on 6p, 5 cases with 6p gain, and 12 cases with 6p12-p21 amplification. A representative ratio profile of case OS-204 showing the amplification of 6p12-p21 is shown in Fig. 1B. We found that most of the cases with amplification of 6p12-p21 displayed increased copy number across the entire region. We defined the common region of amplification to a 7.9 Mb region at 6p12-p21 encompassing RP11-91E11 to RP1-244F24 and identified 10 highly amplified clones from this region (Fig. 2).

### Transcript Analysis of Genes that Are Amplified at 6p12-p21 in Osteosarcoma Cell Lines and Primary Tumors

The common region of amplification contains ~261 known genes spanning 7.9-Mb region on the 6p12-p21 region. We selected 11 candidate genes from the amplified clones based on their cancer-related function such as cell proliferation, transformation, apoptosis, genomic instability, and cell adhesion using the gene information available from the Ensembl genome data resource, National Center for Biotechnology Information, and the University of California at Santa Cruz (Fig. 3A). To assess whether the observed DNA copy number increase in the region encompassing *MAPK14*, *MAPK13*, *CDKN1A*, *PIM1*, *MDGA1*, *BTB9*, *DNAH8*, *CCND3*, *PTK7*, *CDC5L*, and *RUNX2* corresponds to increased levels of one or more of these transcripts, qRT-PCR analysis of 11 genes encoded in the 6p12-p21 amplicon was done on 13 primary tumors and 7 osteosarcoma cell lines, using nonmalignant human osteoblast cells (NHOS) as a control reference. Only 3 of 11 genes, *CCND3*, *CDC5L*, and *RUNX2*, showed consistent overexpression in all osteosarcoma patient samples studied (13 of 13). In contrast, *MAPK14*, *MAPK13*, *CDKN1A*, *PIM1*, *MDGA1*, *BTB9*, and *PTK7* were underexpressed (Fig. 3B). Array CGH data is available for 4 of the 13 cases. Of these, all 4 cases exhibited increased DNA copy number for *MAPK14*, *MAPK13*, *CDKN1A*, *PIM1*, *MDGA1*, *BTB9*, and *PTK7*. In two cases (OS-449, OS-568), the overexpression of *CCND3*, *CDC5L*, and *RUNX2* was not associated with an increase in DNA copy number (Table 1). This suggests that additional alterations, including insertions/rearrangements or epigenetic changes other than amplification, may lead to the overexpression of these genes. The expression pattern of *CCND3*, *CDC5L*, and *RUNX2* was variable in seven osteosarcoma cell lines analyzed. Of these three genes, *CDC5L* and *RUNX2* were overexpressed in MG-63, CRL-1543, MNNG, U2OS, CRL-8304, CRL-11226 and CRL-7631, CRL-7642, CRL-1543, MNNG, SAOS2, U2OS, respectively (Fig. 3C). The expression pattern of *CCND3* is <2-fold higher than the control in all cell lines tested.

### Increased *CDC5L* Transcripts Are Associated with Elevated Levels of *CDC5L* Protein in Osteosarcoma Cell Lines and Primary Tumors

To assess whether increased *CDC5L*, *RUNX2*, and *CCND3* transcripts result in increased levels of protein, Western blot analysis was done on seven osteosarcoma cell lines (Fig. 4A). In

general, CDC5L protein was overexpressed compared with CCND3 and RUNX2 (Fig. 4B). Overexpression of CDC5L protein was noted in four of the seven cell lines (MNNG, MG63, CRL-7543, and U2OS) studied. Of these cell lines, MG63 and MNNG cells showed high-level expression (>10-fold) of CDC5L followed by U2OS and CRL-7543 (>8-fold). Interestingly, all four cell lines also overexpressed *CDC5L* transcripts. The expression level of RUNX2 was higher than CCND3 in all the cell lines tested and SAOS2 cells showed the highest-level expression of RUNX2 (>6 fold).

The protein expression levels of CDC5L, RUNX2, and CCND3 were also analyzed by immunohistochemistry on sections from six individual cases (196, 223, 226, 355, 361, and 363) and osteosarcoma-specific tissue microarrays with 52 cases (Fig. 4C). To define the distribution of CDC5L, RUNX2, and CCND3 immunopositivity on osteosarcoma sections, average intensity scores were calculated for each tumor. Based on the intensity scores, we classified tumors into low, medium, and high expressing groups. Consistent with Western blot analysis, high expression of CDC5L is noted in >23% of tumors compared with RUNX2 (~8%; Fig. 4D). None of the cases showed high expression levels of CCND3.

### Oncogenic Activity of CDC5L

We used an *in vivo* assay to show that CDC5L possesses potential oncogenic activity. In this assay, NIH3T3 cells expressing transfected CDC5L show the ability to form malignant tumors in severe combined immunodeficient mice when compared with the controls (nontransfected NIH3T3 cells). NIH3T3 cells were stably transfected with mouse *CDC5L* cDNA in a myc epitope—tagged vector (pCS2MT). After initial screening, we selected two clones (nos. 1 and 5) based on their differing levels of CDC5L expression (Fig. 5). Tumorigenicity was assayed by inoculating severe combined immunodeficient mice with different numbers of cells from clones 1 and 5 in the supraclavicular region. After 2 to 3 weeks of inoculation, both clones developed tumors at the site of inoculation (Fig. 6A). These tumors exhibited high-level expression of CDC5L and complex chromosomal rearrangements, assayed by Western blot and spectral karyotypic (SKY) analysis, respectively (Figs. 6B and 7). The SKY analysis identified a karyotype 43-67,XX,Rb(1;1),Dup(4),Rb(6;12),-Der(6)T(6;12)(B1;B2),+7,+9,+10,-11,-12,+13, Del(14)(C3),+14,+15,-16,-17,-18,-18,-19[cp5] in the genomic complement of tumor obtained from clone 1 (Fig. 7). The spectral analysis from clone 5 revealed a karyotype of 60-65,XX,-1,Dup(4),Der(6)T(6;12)(B1;B2),+6,Del(14)(C3), Del(15)(A2),+15,+15,+17 [cp10] (Fig. 7).

### Discussion

Osteosarcomas are characterized by a high incidence of chromosomal amplifications and rearrangements (2-8,10). Our previous study using 1-Mb arrays in osteosarcoma refined amplification boundaries for several recurrent chromosomal amplifications identified by CGH, including a 6p amplicon (10). This previous study did not define the exact amplicon boundaries or identify possible target gene(s) from the 6p12-p21 amplicon due to low-density clone coverage on 6p. Therefore, we carried out a systematic evaluation to identify putative oncogene(s) from the 6p12-p21 amplicon. Based on our region-specific array CGH analysis on primary osteosarcoma tumors, we refined the amplicon to 7.9 Mb on 6p and identified 10 highly amplified clones. Subsequently, we identified 11 candidate genes within the amplified clones.

A comprehensive expression analysis of these genes was carried out on primary osteosarcoma tumors and cell lines based on the concept that the amplification leads to the overexpression of genes. Our expression data revealed a consistent overexpression of *CCND3*, *CDC5L*, and *RUNX2* in primary tumors and cell lines. Of these three genes, *CCND3* has been previously implicated in several tumor types (13,15-19). *CCND3* is a member of a family with cyclin D, which encodes a protein involved in the regulation of the G<sub>1</sub>-S phase of cell cycle regulation.

Recently, Kasugai et al. (13) identified *CCND3* and *BYSL* as the targets for the 6p21 amplification in diffuse large cell lymphoma. Similarly, co-overexpression of *EMSI* gene with *CCND1* with 11q13 amplification has been reported in several tumor types (15-19). *RUNX2* is a transcription factor that regulates bone development and belongs to one of three members (*Runx1/AML* and *Runx3*) of the runt family (20). It seems that *RUNX2* coordinates terminal cell cycle exit through the induction of the CDK2 inhibitor, p27/KIP1, which is required for normal bone development *in vitro* and *in vivo* (21). Although *RUNX2* has not yet been implicated in human cancers, *RUNX2* oncogenic activity has been shown in mice. Retroviral insertion studies indicate that *RUNX2* may cooperate with c-myc to promote lymphomas in transgenic mice (22). *CDC5L* is a transcriptional regulator that has homology with the *Saccharomyces pombe cdc5* gene product and contains two tandem repeats of a helix-turn-helix DNA-binding motif with similarity to Myb-related proteins (23-25). Bernstein and Coughlin (25) showed that overexpression of *CDC5L* leads to shorter G<sub>2</sub> phase and reduced cell size in mammalian cells. Interestingly, cell cycle proliferating signature genes (*PLK1*, *CCNE1*, *CCND1*, and *CCNB1*) identified by microarray analysis have recently been implicated in cancer diagnostics. This study substantiates the critical role of cell cycle regulatory genes in cancer biology and clinical management of the patients (26). Recent cDNA microarray studies on three cell lines and three primary osteosarcomas identified the overexpression of *HSPCB* (27).

Further, we investigated whether increased DNA copy number and overexpression of *CCND3*, *CDC5L*, and *RUNX2* transcripts correlate with increased protein levels in osteosarcoma cell lines and tissue microarrays by Western blot analysis and immunohistochemistry, respectively. According to our protein expression data, *CDC5L* protein overexpression is more frequent than *RUNX2* and *CCND3*, indicating the pivotal role of *CDC5L* in osteosarcoma pathogenesis. Finally, we used an *in vivo* tumorigenesis assay to show the oncogenic nature of *CDC5L*.

Taken together, these findings strongly suggest *CDC5L* as the target for 6p12-p21 amplification found in osteosarcoma. Overexpression of *CDC5L* through genomic gain/amplification is likely to lead to aberrant cell cycle control and may contribute to the malignant phenotype in osteosarcoma. Therefore, identification of genes regulated by *CDC5L* will shed light not only on the precise mechanism by which *CDC5L*-like proteins regulate cell cycle progression, specifically the G<sub>2</sub>-M transition, but is also likely to provide vital insight into the molecular mechanisms of the development of malignancy. Critically, inhibitors of *CDC5L* function might prove useful for arresting cell proliferation in osteosarcoma.

## Materials and Methods

### Patient Samples and Cell Lines

Thirty-six tumors from 26 patients (14 males and 12 females) were collected from the Texas Children's Cancer Center, Houston, TX (tumors OS-196, OS-197, OS-204, OS-223, OS-226, OS-248, OS-274, OS-285, OS-295, OS-307, OS-311, OS-355, OS-361, OS-363, OS-364, OS-394, OS-400, OS-425, OS-449, OS-464, OS-501, OS-527, OS-568, OS-589, OS-606, and OS-656) and Memorial Sloan Kettering Cancer Center, New York, NY (tumors OS-13, OS-46, OS-27L, OS-68L, OS-76L, OS-79L, OS-80L, OS-82L, OS-88L, and OS-161). All tissues in this study were obtained after institutional review board—approved informed consents were signed. Seven osteosarcoma cell lines (U2OS, SAOS2, MG-63, MNNG, CRL-7543, CRL-7631, and CRL-7642) and NHOS were purchased from the American Type Culture Collection and were grown according to the supplier's recommendations.

## Region-Specific Array CGH

The region-specific array used in this study was generated using 108 human BAC and PAC clones spaced ~0.26 Mb apart across a 28.8 Mb region spanning 6p12-p21. Twenty-four additional clones covering the chromosome 6 region and 16 clones from other autosomes were also used. Thirty-eight clones from chromosome X, 20 clones from 6pter-p22, 4 clones from 6q, and clones from other autosomes were used as internal controls. A total of 60 autosomal clones were mixed and printed at four different concentrations (25, 50, 75, and 100 ng/ $\mu$ L) for data normalization.

The arrays were made by directly printing the neutralized modified BAC/PAC DNA solution onto acid-cleaned plain glass slides using the Qarray mini Arrayer from Genetix and each clone is spotted in triplicate. Arrays were prehybridized with human Cot-1 DNA (Life Technologies) and salmon testes DNA to block the repetitive sequences on BACs. One microgram of normal DNA (reference) and tumor DNA (test) was labeled with cy5-dUTP and cy3-dUTP, respectively, by random priming. To avoid dye bias, we did dye swap experiments for each sample. The probe mixture was dissolved in hybridization mixture, denatured, cooled, and mounted with a 22  $\times$  60 mm coverslip. Hybridizations were done in sealed chambers for 16 to 20 h at 37°C. After posthybridization washes, arrays were dried with compressed air and scanned into two 16-bit TIFF image files using Gene Pix 4000A two-color fluorescent scanner (Axon Instruments, Inc.) and quantitated using GenePix software (Axon Instruments). After scanning the slide, the median fluorescent intensity values of pixels around each spot were subtracted from the median fluorescent intensity value of each spot. A fixed distance of 5 pixels from the periphery of each spot was used to calculate the background intensity values. Each of the background-subtracted values can now be used to compute the ratio of the red and green channels. The resulting values were normalized by using the linear regression method with in-house control DNA spots to correct for systematic bias in dye labeling and fluorescent intensity. The ratio of the red/green channel of each clone was calculated, which reflects the changes in DNA sequence copies. Each experiment was repeated once with dye reversal to address the confounding effect of the dye and the experiment. The average of the dye reversal experiment pair was calculated by reversing the sign of one experiment so that the log ratio reflects the tumor versus normal ratio. The candidate genes were identified within the amplified BAC clones from 6p12-p21 using the gene information available from the Ensemble genome data resource,<sup>8</sup> the National Center for Biotechnology Information cancer gene map,<sup>9</sup> and the University of California at Santa Cruz Biotechnology.<sup>10</sup>

## Quantitative Real-time RT-PCR

Total RNA was extracted from NHOS (American Type Culture Collection), osteosarcoma patient tissue samples (OS-13, OS-46, OS-161, OS-204, OS-248, OS-274, OS-295, OS-361, OS-449, OS-568, OS-589, OS-606 and OS-656), and seven cell lines using the Strataprep Total RNA microprep kit (Stratagene). Total RNA was treated with 2 to 10 units of RNase-free DNase I (Promega). cDNA synthesis was done by reverse transcription of 2  $\mu$ g of total RNA using a cocktail of random hexamers and oligo dT<sub>12-18</sub> primer. Beacon Designer 2.0 software (Premier BioSoft International) was used to design all primers. The primer information is summarized in Table 2. Real-time PCR was done for MAPK14, MAPK13, CDKN1A, PIM1, MDGA1, BTB9, DNAH8, CCND3, PTK7, CDC5L, and *RUNX2* using the iCycler system (Bio-Rad Laboratories) in a two-step reaction. Copy numbers were internally normalized to glyceraldehyde 3-phosphate dehydrogenase (Genbank M32599) expression and quantitated relative to the NHOS cell line. Results from at least three separate experiments were analyzed.

<sup>8</sup><http://www.ensembl.org/genome/central/>

<sup>9</sup><http://www.ncbi.nlm.nih.gov/>

<sup>10</sup><http://genome.ucsc.edu/cgi-bin/hgGateway?org=human>

Results of the RT-PCR analysis are expressed as  $C_t$  values, which are used to determine the amount of target gene mRNA relative to the amount of reference gene mRNA.

### Western Blot Analysis

The protein lysates were prepared from NHOS and seven osteosarcoma cell lines using previously published protocol (28). Cell pellets were lysed in radioimmunoprecipitation assay buffer (PBS, 1% NP40, 0.1% SDS, 0.5% sodium deoxycholate) or PBSTDS buffer (PBS, 1% Triton X-100, 0.1% SDS, 0.5% sodium deoxycholate) containing protease and phosphatase inhibitors (1 mmol/L EDTA, 0.2 mmol/L phenylmethylsulfonyl fluoride, 1  $\mu$ g pepstatin/mL, 30  $\mu$ L aprotinin/mL, 0.5  $\mu$ g leupeptin/mL, and 100 mmol/L sodium orthovanadate and 100 mmol/L sodium fluoride) for 10 to 15 min on ice, followed by passage through a 21G needle. When appropriate, additional phosphatase inhibitors, cocktail I and II (Sigma-Aldrich), were added to the lysis buffer at a dilution of 1:100. Lysates were then centrifuged at  $1,000 \times g$  for 20 min, and the supernatants were aliquoted and frozen at  $-80^\circ\text{C}$  until use. After protein quantification (using detergent compatible protein dye and bovine serum albumin standards from Bio-Rad) and normalization, 30 to 40  $\mu$ g of protein extracts were electrophoresed on SDS-PAGE gels and transferred to polyvinylidene difluoride membranes (Millipore). The filters were initially blocked with Li-Cor Odyssey Blocking Buffer for 1 to 2 h at room temperature and then probed with CDC5L (1:500), RUNX2 (1:200), CCND3 (1:500), and  $\beta$ -actin antibodies (1:100,000). The antibodies for CDC5L, RUNX2, and CCND3 were purchased from BD Biosciences, R&D Systems, and Santa Cruz Biotechnology, respectively. The bound primary antibodies were detected with IRD800 dye—labeled appropriate species-specific secondary antisera and signal was visualized on a Li-Cor Odyssey IR scanner.

### Immunohistochemical Analysis

Immunohistochemical analysis was done for CCND3, RUNX2, and CDC5L on seven formalin-fixed, paraffin-embedded tissue sections from TXCCC (196, 223, 226, 355, 361, and 363) and tissue microarray consisting of 55 unique osteosarcoma cases (Cooperative Human Tissue Network) using standard techniques. Briefly, sections were deparaffinized in xylene, rehydrated in decreasing ethanol from 100% to 75%, microwaved for  $3 \times 3$  min in 10 mmol/L citrate buffer (pH 6.0) at  $95^\circ\text{C}$  to  $99^\circ\text{C}$  for antigen retrieval, and finally endogenous peroxidase activity was quenched with 3% hydrogen peroxide at room temperature. Nonspecific binding was blocked by incubating sections in PBS-T with 10% normal horse serum for 30 min at room temperature. Tissue sections were incubated overnight at  $4^\circ\text{C}$  with an appropriate antibody for CCND3 (1:20), RUNX2 (1:50), and CDC5L (1:100). After four PBS washes with 0.1% Tween 20 for 2 h, sections were incubated with horseradish peroxidase—conjugated streptavidin using the Vectastin Elite ABC kit (Vector Laboratories, Inc.) for 45 min at room temperature. Peroxidase activity was revealed with 3',3'-diaminobenzidine tetrahydrochlorate using a 3',3'-diaminobenzidine kit (Vector Laboratories) according to the protocol provided. Finally, sections were washed in distilled water for terminating the reaction, counterstained with hematoxylin, and mounted.

### Oncogenic Activity of CDC5L

The NIH/3T3 cell line was obtained from the American Type Culture Collection and maintained per American Type Culture Collection protocol. Cells were transfected with 2.5  $\mu$ g of pCS2MT-cdc5L along with neomycin-resistant pCRUZ-HA plasmid DNA (for drug selection), using PolyFect transfection reagent (Qiagen). Empty vectors (2.5  $\mu$ g of pcs2MT and pCRUZ-HA) were used as controls. Forty-eight hours later, 200  $\mu$ g/mL of G418 were added to select the stable transfectants, which was continued for 3 wk. At the end of the 3rd week, 100 stable clones were isolated and expanded. Levels of myc-Cdc5L expression in the

selected clones were examined using Western blot analysis with hcdc5L monoclonal antibody and myc epitope tag monoclonal antibody (9E10).

From the screen, clones 1 and 5 were selected based on their varying levels of expression of CDC5L. We also selected clone 105EV with empty vectors as a control. We injected  $>5 \times 10^6$  cells from each of clone (nos. 1 and 5) and 105EV to each 8-wk-old male severe combined immunodeficient mouse. The appearance of tumors in the mice was monitored twice a week using palpation. Following 2 wk of injection, all five of the clone 5—injected mice developed tumors, whereas at the end of 3 wk, all the mice from clone 1 showed the presence of tumors. The mice were sacrificed at the end of 4 wk for clone 5 and at 6 wk for clone 1 due to high tumor burden. Tumors were harvested and subjected to Western blot and SKY analysis of the tumor specimens to examine the CDC5L protein expression and chromosomal changes, respectively. However, there were no sign of tumors in the control mice until 5 wk of injection. At 6th week, 4 of 5 mice showed palpable tumors from control group injected with empty vector. These tumors were extremely slow growing. Such tumors arising from NIH3T3 cells injected to severe combined immunodeficient mice was previously been reported (29). Mice were sacrificed at 10 wk following injection and tumors were harvested.

### Spectral Karyotypic Analysis

The cocktail of mouse chromosome paints was obtained from Applied Spectral Imaging. Hybridization and detection were carried out according to the manufacturer's protocol, with slight modifications. Chromosomes were counterstained with 4',6-diamidino-2-phenylindole. For each case, 5 to 10 metaphase cells were analyzed by SKY. Images were acquired with a SD200 Spectra cube (Applied Spectral Imaging) mounted on a Zeiss Axioplan II microscope using a custom-designed optical filter (SKY-1; Chroma Technology) and analyzed using SKY View 2.1.1 software (Applied Spectral Imaging).

### Acknowledgments

**Grant support:** National Childhood Cancer Foundation (Alex Lemonade Stand Funds; P.H. Rao), Dunn Foundation, Kleberg Foundation CA88126, CA114757 (C.C. Lau), and National Cancer Institute grant 1R01 CA109330 (D. Pati).

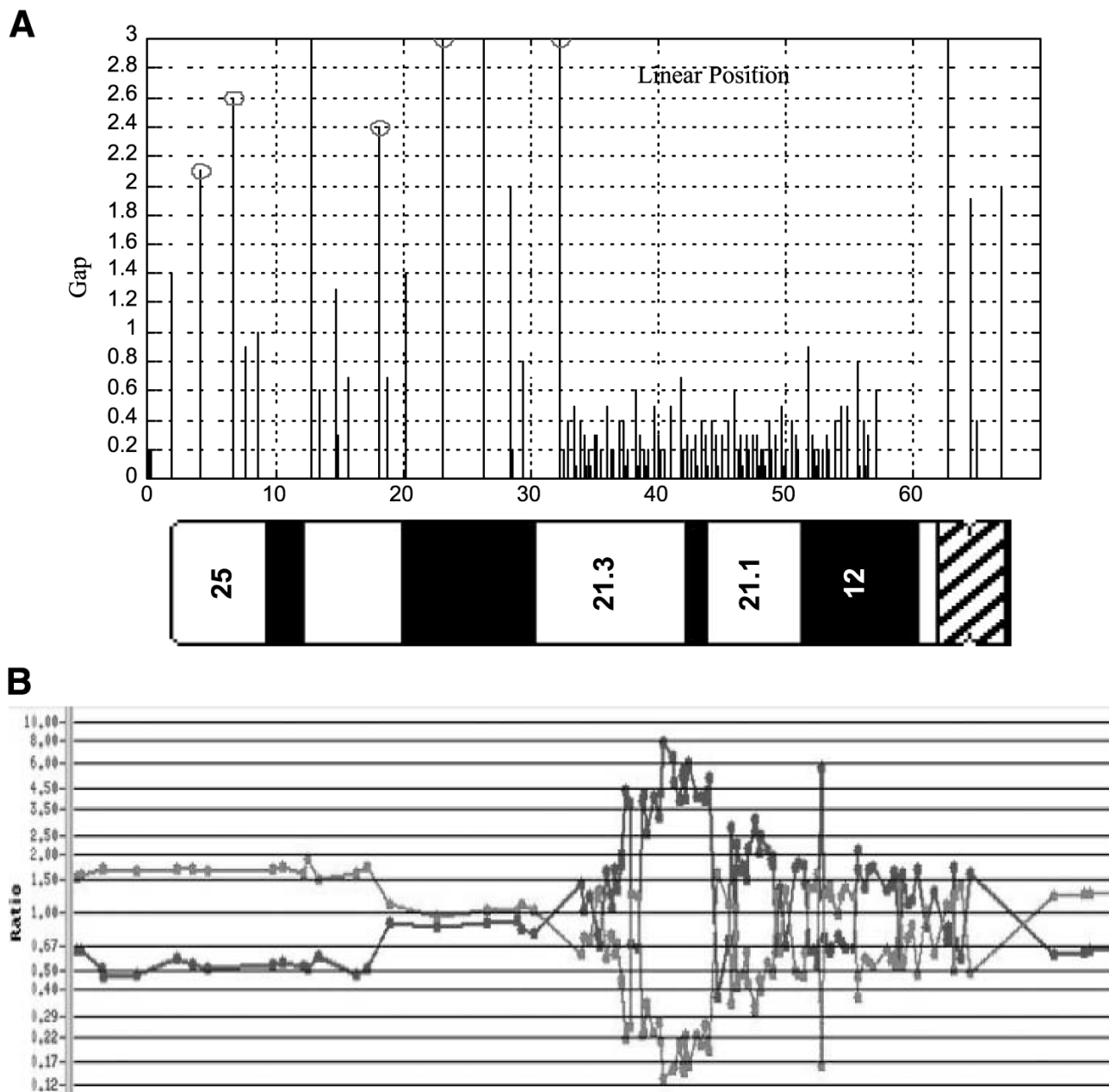
### References

1. Spina V, Montanari N, Romagnoli R. Malignant tumors of the osteogenic matrix. *Eur J Radiol* 1998;27 (Suppl 1):S98–109. [PubMed: 9652509]
2. Tarkkanen M, Karhu R, Kallioniemi A, et al. Gains and losses of DNA sequences in osteosarcomas by comparative genome hybridization. *Cancer Res* 1995;55:1334–38. [PubMed: 7882332]
3. Forus A, Weghuis DO, Smeets D, et al. Comparative genomic hybridization analysis of human sarcomas: II. Identification of novel amplicons at 6p and 17p in osteosarcomas. *Genes Chromosomes Cancer* 1995;14:15–21. [PubMed: 8527379]
4. Tarkkanen M, Elomaa I, Blomqvist C, et al. DNA sequence copy number increase at 8q: a potential new prognostic marker in high-grade osteosarcoma. *Int J Cancer* 1999;84:114–21. [PubMed: 10096241]
5. Stock C, Kager L, Fink F-M, Gadner H, Ambros PF. Chromosomal regions involved in the pathogenesis of osteosarcoma. *Genes Chromosomes Cancer* 2001;28:329–36. [PubMed: 10862039]
6. Zielenska M, Bayani J, Pandita A, et al. Comparative genomic hybridization analysis identifies gains of 1p35-36 and chromosome 19 in osteosarcoma. *Cancer Genet Cytogenet* 2001;130:14–21. [PubMed: 11672768]
7. Overholtzer M, Rao PH, Favis R, et al. The presence of p53 mutations in human osteosarcomas correlates with high levels of genomic instability. *Proc Natl Acad Sci U S A* 2003;100:11547–52. [PubMed: 12972634]



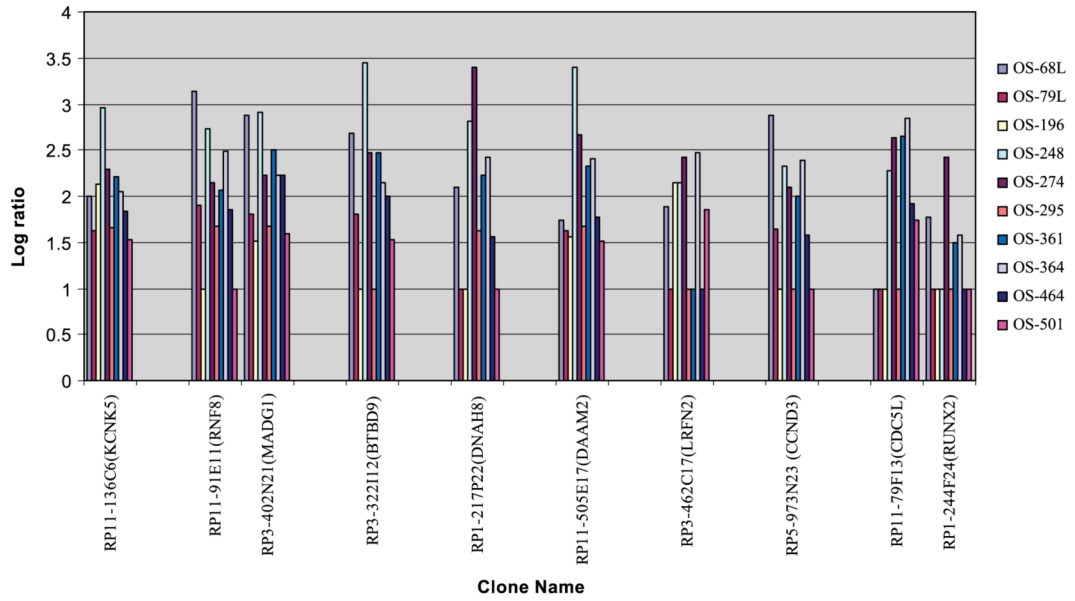
8. Lau CC, Harris CP, Lu XY, et al. Frequent amplification and rearrangement of chromosomal bands 6p12-21 and 17p11.2 in osteosarcoma. *Genes Chromosomes Cancer* 2004;39:11–21. [PubMed: 14603437]
9. Weatherby RP, Dahlin DC, Ivins JC. Postradiation sarcoma of bone: review of 78 Mayo Clinic cases. *Mayo Clin Proc* 1981;56:294–306. [PubMed: 6939953]
10. Man TK, Lu XY, Jaeweon K, et al. Genome-wide array comparative genomic hybridization analysis reveals distinct amplifications in osteosarcoma. *BMC Cancer* 2004;4:45. [PubMed: 15298715]
11. Bruch J, Schulz WA, Häussler J, et al. Delineation of the 6p22 amplification unit in urinary bladder carcinoma cell lines. *Cancer Res* 2000;60:4526–30. [PubMed: 10969802]
12. Heidenblad M, Schoenmakers EF, Jonson T, et al. Genome-wide array-based comparative genomic hybridization reveals multiple amplification targets and novel homozygous deletions in pancreatic carcinoma cell lines. *Cancer Res* 2004;64:3052–59. [PubMed: 15126341]
13. Kasugai Y, Tagawa H, Kameoka Y, Morishima Y, Nakamura S, Seto M. Identification of CCND3 and BYSL as candidate targets for the 6p21 amplification in diffuse large B-cell lymphoma. *Clin Cancer Res* 2005;11:8265–72. [PubMed: 16322284]
14. Orlic M, Spencer CE, Wang L, Gallie BL. Expression analysis of 6p22 genomic gain in retinoblastoma. *Genes Chromosomes Cancer* 2006;45:72–82. [PubMed: 16180235]
15. Schuurin E, Verhoeven E, Mooi WJ, Michalides RJ. Identification and cloning of two overexpressed genes, U21B31/PRAD1 and EMS1, within the amplified chromosome 11q13 region in human carcinomas. *Oncogene* 1992;7:355–61. [PubMed: 1532244]
16. Bringuier PP, Tamimi Y, Schuurin E, Schalken J. Expression of cyclin D1 and EMS1 in bladder tumours; relationship with chromosome 11q13 amplification. *Oncogene* 1996;12:1747–53. [PubMed: 8622895]
17. van Damme H, Brok H, Schuurin-Scholtes E, Schuurin E. The redistribution of cortactin into cell-matrix contact sites in human carcinoma cells with 11q13 amplification is associated with both overexpression and post-translational modification. *J Biol Chem* 1997;272:7374–80. [PubMed: 9054437]
18. Yuan BZ, Zhou X, Zimonjic DB, Durkin ME, Popescu NC. Amplification and overexpression of the EMS1 oncogene, a possible prognostic marker, in human hepatocellular carcinoma. *J Mol Diagn* 2003;5:48–53. [PubMed: 12552080]
19. Rodrigo JP, Garcia LA, Ramos S, Lazo PS, Suarez C. EMS1 gene amplification correlates with poor prognosis in squamous cell carcinomas of the head and neck. *Clin Cancer Res* 2000;6:3177–82. [PubMed: 10955801]
20. Blyth K, Cameron ER, Neil JC. The RUNX genes: gain or loss of function in cancer. *Nat Rev Cancer* 2005;5:376–87. [PubMed: 15864279]
21. Thomas DM, Johnson SA, Sims NA, et al. Terminal osteoblast differentiation, mediated by runx2 and p27KIP1, is disrupted in osteosarcoma. *J Cell Biol* 2004;167:925–34. [PubMed: 15583032]
22. Stewart M, Terry A, Hu M, et al. Proviral insertions induce the expression of bone-specific isoforms of PEBP2 $\alpha$ A (CBFA1): evidence for a new myc collaborating oncogene. *Proc Natl Acad Sci U S A* 1997;94:8646–51. [PubMed: 9238031]
23. Nasmyth K, Nurse P. Cell division cycle mutants altered in DNA replication and mitosis in the fission yeast *Schizosaccharomyces pombe*. *Mol Gen Genet* 1981;182:119–24. [PubMed: 6943408]
24. Ohi R, McCollum D, Hirani B, et al. The *Schizosaccharomyces pombe* cdc5+ gene encodes an essential protein with homology to c-Myb. *EMBO J* 1994;13:471–83. [PubMed: 8313892]
25. Bernstein HS, Coughlin SR. A mammalian homolog of fission yeast Cdc5 regulates G<sub>2</sub> progression and mitotic entry. *J Biol Chem* 1998;273:4666–71. [PubMed: 9468527]
26. Whitfield ML, George LK, Grant GD, Perou CM. Common markers of proliferation. *Nat Rev Cancer* 2006;6:99–106. [PubMed: 16491069]
27. Wolf M, El-Rifai W, Tarkkanen M, et al. Novel findings in gene expression detected in human osteosarcoma by cDNA microarray. *Cancer Genet Cytogenet* 2000;123:128–32. [PubMed: 11156738]
28. Pati D, Zhang N, Plon SE. Linking sister chromatid cohesion and apoptosis: role of Rad21. *Mol Cell Biol* 2002;22:8267–77. [PubMed: 12417729]

29. Sutherland BM, Bennett PV, Freeman AG, Moore SP, Strickland PT. Transformation of human cells by DNAs ineffective in transformation of NIH 3T3 cells. Proc Natl Acad Sci U S A 1985;82:2399–403. [PubMed: 3857589]

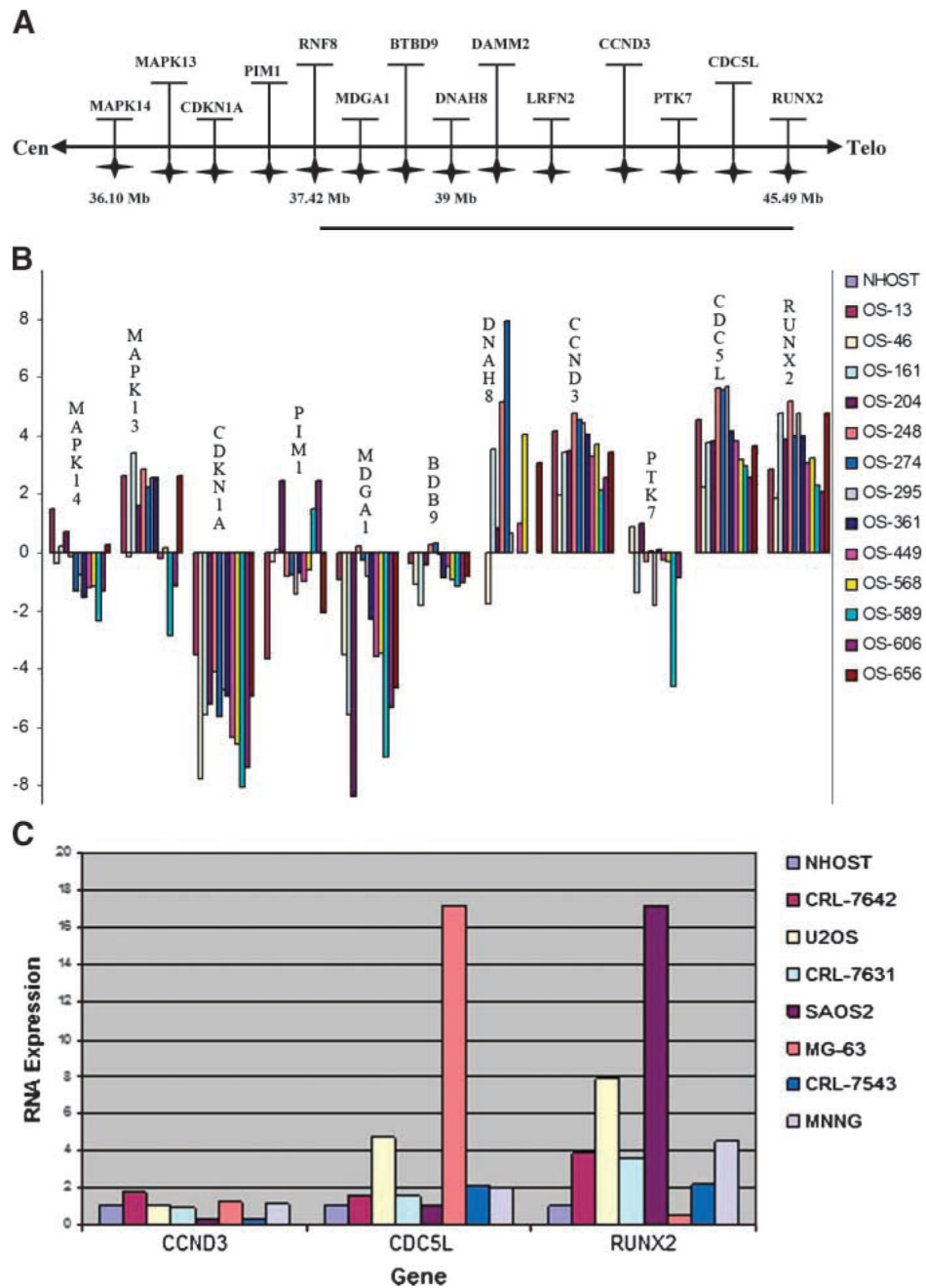


**FIGURE 1.**

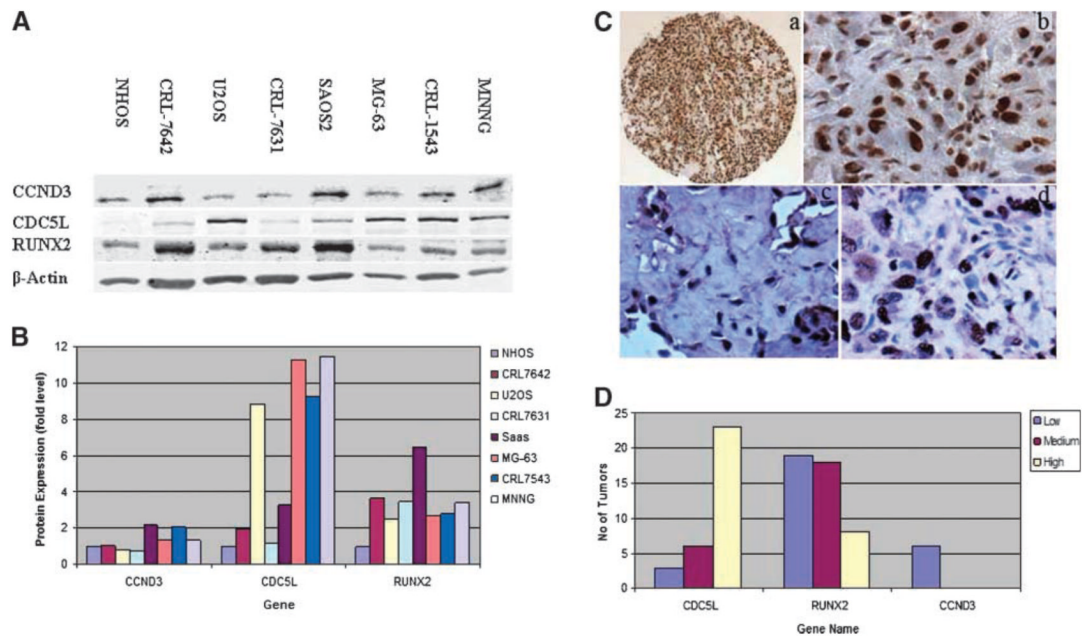
**A.** Partial 6p ideogram with a contig of BAC/P1 clones used to generate region-specific array. Each bar represents a BAC/PAC clone. **B.** A representative region-specific ratio profile of 6p12-p21 from case OS-204. In this experiment, tumor and normal DNA were labeled with Cy5 and Cy3, respectively. The dye reversal experiment was also done to avoid dye biases and hybridization artifacts. The mean ratios were plotted along the length of the chromosome. The clones on each chromosome are arranged (pter to qter) based on University of California at Santa Cruz mapping positions.

**FIGURE 2.**

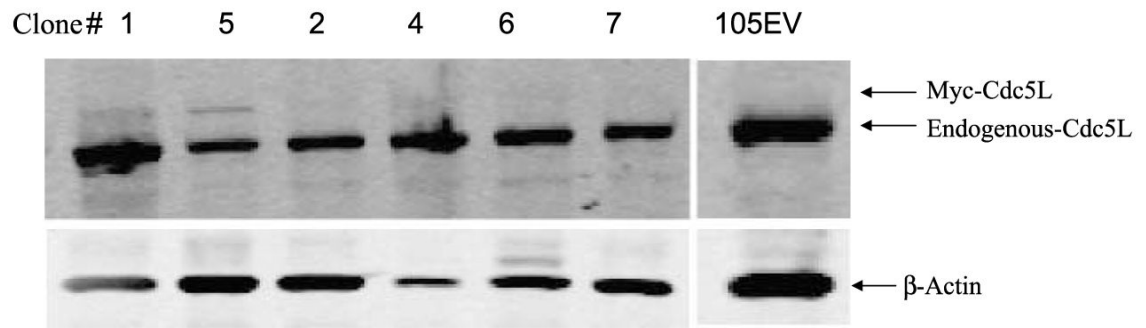
Amplicon mapping of 6p12-p21 in osteosarcoma. Log ratios of 10 BAC clones around the highly amplified region. All the clones are arranged (pter to qter) based on University of California at Santa Cruz mapping positions.

**FIGURE 3.**

**A.** The genes within the amplified BAC/P1 clones are arranged from centromeric to telomeric on 6p12-p21 region. **B.** Quantitative RT-PCR for MAPK14, MAPK13, CDKN1A, PIM1, MDGA1, BTBD9, DNAH8, CCND3, PTK7, CDC5L, and *RUNX2* was done on 13 primary osteosarcoma tumors. The results are displayed as fold RNA expression normalized to NHOST. **C.** Quantitative RT-PCR was done for *CCND3*, *CDC5L*, and *RUNX2* on seven osteosarcoma cell lines. The results are displayed as fold RNA expression normalized to NHOST.

**FIGURE 4.**

**A.** Western blot analysis of CCND3, CDC5L, and RUNX2 protein expression in a panel of seven osteosarcoma cell lines and NHOS. Human  $\beta$ -actin was used as loading control. **B.** Expression of CCND3, CDC5L, and RUNX2 as fold increases over NHOS after normalization to the expression of a housekeeping gene  $\beta$ -actin to compare for loading control. **C.** Immunohistochemistry analysis on osteosarcoma tumor sections using antibodies for CDC5L (a, b), CCND3 (c), and RUNX2 (d). **D.** Protein expression frequency (low, medium, and high) of CCND3, CDC5L, and RUNX2 in tissue microarray sections from patients with osteosarcoma.

**FIGURE 5.**

Western blot analysis of CDC5L protein in stably transfected NIH/3T3 cell clones. Expression of myc-epitope — tagged CDC5L and endogenous CDC5L protein was examined using 9E—10 and hCdc34 monoclonal antibody, respectively. Clone 105EV is an empty vector clone used as a negative control and  $\beta$ -actin is shown as loading control.

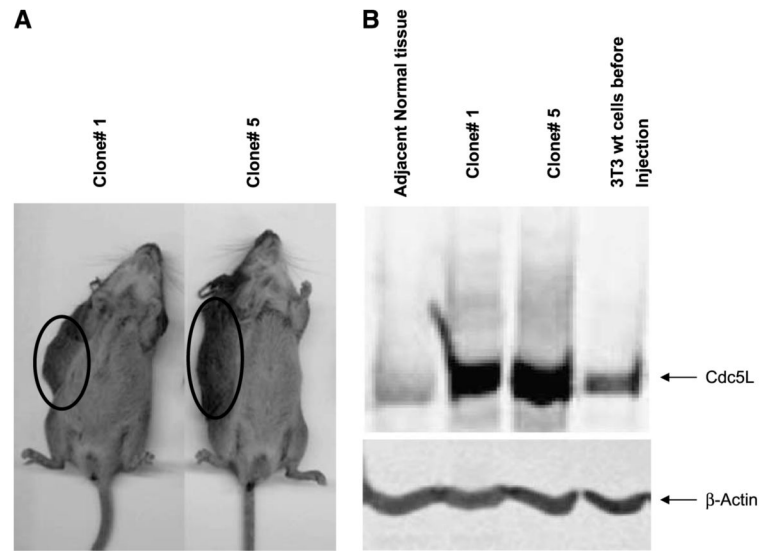


**FIGURE 6.** Oncogenic nature of *CDC5L*. **A.** The severe combined immunodeficient mice developed tumors after inoculation of transfected NIH/3T3 cells with clones 1 and 5 in the supraclavicular region. **B.** The Western blot analysis of tumors developed from transfection showing increased level of *CDC5L* protein compared with NIH/3T3 cells and normal adjacent tissue.



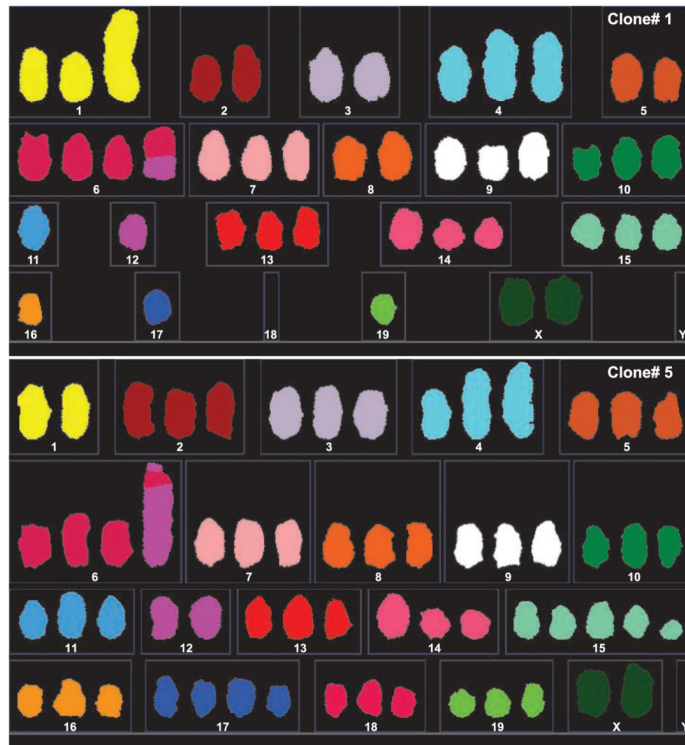


**FIGURE 7.** Multicolor spectral karyotypic analysis of tumors derived from clones 1 and 5 showing classification colors. Both karyo-types were characterized by multiple chromosomal abnormalities.

**Table 1**  
 Comparison of Amplification and Expression Levels of CCND3, CDC5L, and RUNX2 in Osteosarcoma Patient Samples

Tumor ID	cCGH	6p12-p21 Region-Specific Array			RNA Expression			Immunohistochemistry		
		CCND3	CDC5L	RUNX2	CCND3	CDC5L	RUNX2	CCND3	CDC5L	RUNX2
OS-13	Amp	ND	ND	ND	▲	▲	▲	ND	ND	ND
OS-46	Gain	ND	ND	ND	▲	▲	▲	ND	ND	ND
OS-27L	NC	NC	NC	NC	ND	ND	ND	ND	ND	ND
OS-68L	Amp	Amp	Amp	Amp	ND	ND	ND	ND	ND	ND
OS-76L	NC	NC	NC	NC	ND	ND	ND	ND	ND	ND
OS-79L	Amp	Amp	Amp	Amp	ND	ND	ND	ND	ND	ND
OS-80L	NC	NC	NC	NC	ND	ND	ND	ND	ND	ND
OS-82L	NC	NC	NC	NC	ND	ND	ND	ND	ND	ND
OS-88L	Gain	Gain	Gain	Gain	ND	ND	ND	ND	ND	ND
OS-161	Gain	ND	ND	ND	▲	▲	▲	ND	ND	ND
OS-196 <sup>a</sup>	Amp	—	—	—	ND	ND	ND	—	▲	▲
OS-197	NC	NC	NC	NC	ND	ND	ND	ND	ND	ND
OS-204 <sup>c</sup>	Amp	Amp	Amp	Amp	▲	▲	▲	ND	ND	ND
OS-223	NC	NC	NC	NC	ND	ND	ND	—	▲	▲
OS-226 <sup>c</sup>	Amp	ND	ND	ND	ND	ND	ND	—	▲	—
OS-248	Amp	Amp	Amp	Amp	▲	▲	▲	—	▲	—
OS-274 <sup>b</sup>	Amp	Amp	Amp	Amp	▲	▲	▲	ND	ND	ND
OS-285	NC	Gain	Gain	Gain	▲	▲	▲	ND	ND	ND
OS-295	Amp	Amp	Amp	Amp	▲	▲	▲	ND	ND	ND
OS-307	NC	NC	NC	NC	ND	ND	ND	ND	ND	ND
OS-311	NC	NC	NC	NC	ND	ND	ND	ND	ND	ND
OS-355 <sup>b</sup>	Amp	ND	ND	ND	ND	ND	ND	—	▲	—
OS-361 <sup>b</sup>	Amp	Amp	Amp	Amp	▲	▲	▲	—	▲	—
OS-363 <sup>b</sup>	Amp	ND	ND	ND	ND	ND	ND	—	▲	—
OS-364 <sup>b</sup>	Amp	Amp	Amp	Amp	ND	ND	ND	ND	ND	ND
OS-394	NC	NC	NC	NC	ND	ND	ND	ND	ND	ND
OS-400	Gain	Gain	Gain	Gain	ND	ND	ND	ND	ND	ND
OS-425	Gain	Gain	Gain	Gain	ND	ND	ND	ND	ND	ND

Tumor ID	cCGH	6p12-p21 Region-Specific Array				RNA Expression			Immunohistochemistry		
		CCND3	CDC5L	RUNX2	CCND3	CDC5L	RUNX2	CCND3	CDC5L	RUNX2	
OS-449 <sup>a</sup>	NC	ND	ND	ND	▲	▲	▲	ND	ND	ND	
OS-464 <sup>d</sup>	Amp	Amp	Amp	—	ND	ND	ND	ND	ND	ND	
OS-501 <sup>d</sup>	Amp	Amp	Amp	Amp	ND	ND	ND	ND	ND	ND	
OS-527	Gain	Gain	Gain	Gain	ND	ND	ND	ND	ND	ND	
OS-568	NC	ND	ND	ND	▲	▲	▲	ND	ND	ND	
OS-589	Amp	—	Amp	Amp	▲	▲	▲	ND	ND	ND	
OS-606	Amp	ND	ND	ND	▲	▲	▲	ND	ND	ND	
OS-656	Gain	ND	ND	ND	▲	▲	▲	ND	ND	ND	

NOTE: ▲, overexpression. Superscripts a, b, c, and d refer to tumor samples derived from the same patient.

Abbreviations: cCGH, chromosomal CGH; NC, no change; Amp, amplified; ND, not done.

**Table 2**  
Primer Information of Genes Used for Quantitative RT-PCR

Accession Number	Gene	Sense Primer	Antisense Primer
NM_001315	<i>MAPK14</i>	TTCTGTTGATCCCACTTCACTGT	ACACAGATGCACACACACTAAC
NM_002754	<i>MAPK13</i>	CCCCAGGAAGGATTTCACTCAG	CTTGCCACAGTCTAGCTCCAG
NM_000389	<i>CDKN1A</i>	GACACTGGCCCTCAAATCG	CTCCTTGTTCGGCTGCTAATCA
NM_002648	<i>PIM1</i>	GAGAAAGGAGCCCTGGAGTC	AAATTGTCGGAGACGCGGGAT
NM_153487	<i>MDGA1</i>	GGCTGTGTGGCGTTTCAAAG	TTGGAGACGGTGCACCTCGTA
NM_152733	<i>BTBD9</i>	CCTGCCTCCTTCAATCCGTATC	CTGTCCCCGATTCTCCTACTATTT
NM_001371	<i>DNAH8</i>	CAGCCA CGAACTCAGAAAATG	TCACTCTCAAATAAGTACTGTTCG
NM_001760	<i>CCND3</i>	GCCACTAAGCAGAGGAGGGG	GGGGATGGGTAGGACCAGATC
NM_002821	<i>PTK7</i>	TCCTTCAGTGAGATTGCCAGC	CTAGAGATGTCCTCCCCCTGCC
NM_001253	<i>CDC5L</i>	TCCTTGAAGCTCCTCTCGGC	CATCTCGGTAATTCCTCCATACG
NM_001024630	<i>RUNX2</i>	GCCCCCAAACAGTATCTTGA	GCCTGAAAGTGAGGTTTTAGGC